Evolution of new nonantibody proteins via iterative somatic hypermutation

Lei Wang*, W. Coyt Jackson*, Paul A. Steinbach*, and Roger Y. Tsien*†‡

Departments of *Pharmacology and †Chemistry and Biochemistry and Howard Hughes Medical Institute, University of California at San Diego, La Jolla, CA 92093-0647

B lymphocytes use somatic hypermutation (SHM) to optimize immunoglobulins. Although SHM can rescue single point mutations deliberately introduced into nonimmunoglobulin genes, such experiments do not show whether SHM can efficiently evolve challenging novel phenotypes requiring multiple unforeseeable mutations in nonantibody proteins. We have now iterated SHM over 23 rounds of fluorescence-activated cell sorting to create monomeric red fluorescent proteins with increased photostability and far-red emissions (e.g., 649 nm), surpassing the best efforts of structure-based design. SHM offers a strategy to evolve nonantibody proteins with desirable properties for which a high-through-put selection or viable single-cell screen can be devised.

directed evolution | mPlum | Ramos | red fluorescent protein

Directed protein evolution is one of the most powerful tools to engineer new protein properties not found in natural proteins (1, 2). To search protein sequence space within weeks or months rather than millennia or millions of years for natural selection, large protein diversities need to be iteratively generated and screened very rapidly and efficiently. *In vitro* methods for creating genetic diversity are very powerful but laborious to apply iteratively when screening has to be done on transfected cells or organisms. Each cycle requires generation of a huge number of different mutant genes, transfection into cells (ideally so that each cell receives at most one mutant), screening for improved phenotype, and amplification, recovery, and sequencing of the DNA encoding the best performers. Mutagenesis in intact living cells would avoid repetitive transfection and reisolation of genes, but existing methods normally randomize the entire genome wastefully and often deleteriously rather than focusing on the gene of interest (3). If mammalian cells could autonomously diversify arbitrarily chosen target genes, one could evolve proteins *in situ* and explore much larger sequence spaces for protein engineering and functional studies.

Genetic information is naturally maintained in high fidelity in most cell types. However, when activated by antigens, B lymphocytes in the immune system can specifically mutate Igs through a process called somatic hypermutation (SHM) (4–8). SHM uses activation-induced cytidine deaminase (AID) and error-prone DNA repair to introduce point mutations into the rearranged V regions of Ig at a rate of $\approx 1 \times 10^{-3}$ mutations per base pair per generation, 10^6 times higher than that in the rest of the genome (9). SHM can repair premature stop codons deliberately introduced in non-Ig genes, provided that they are transcribed at a high enough rate (7, 8). However, to revert a single fatal base pair in one step is a far more modest task than to find multiple subtle mutations creating a desirable phenotype never seen before. We demonstrate here that SHM could generate useful phenotypes from a foreign gene. The gene for a monomeric red fluorescent protein (mRFP), *mRFP1.2* (10), was expressed in the Burkitt lymphoma Ramos, a human B cell line that hypermutates its Ig V genes constitutively during culture (11). mRFP mutants with enhanced photostability and far-red emissions were evolved through iterative SHM and fluorescence-activated cell sorting (FACS).

Materials and Methods

Introduction of the *mRFP1.2* Gene into Ramos Cells. The *mRFP1.2* gene was amplified with primer pair LW5 (5′-CGCGGATC-CGCCACCATGGTGAGCAAGGGC-3′) and LW3 (5′-CCATCGATTTAGGCGCCGGTGGAGTGGCG-3′), digested with *Bam*HI and *Cla*I, and ligated into a precut pCLNCX (Imgenex, San Diego) derivative retroviral vector, in which the cytomegalovirus (CMV) promoter was replaced with the inducible Tet-on promoter. The resultant plasmid, pCLT-mRFP, was cotransfected with pCL-Ampho (Imgenex) into HEK293 cells to make the retrovirus, which was subsequently used to infect Ramos cells [CRL-1596, American Type Culture Collection (ATCC)] together with another retrovirus harboring the reverse Tet-controlled transactivator. Ramos cells were grown in modified RPMI medium 1640 as suggested by ATCC. Doxycycline (2 μg/ml) was added to induce the expression of mRFP 24 h before FACS, and infected cells were sorted for six rounds to enrich red fluorescent cells. In the initial sorting, <5% of cells became red, indicating a multiplicity of infection well below 1.

Protein Evolution by FACS. Ratio sorting was applied to evolve mRFP mutants with red-shifted emissions. Ramos cells were excited at 568 nm, and two emission filters (660/40 and 615/40) were used. The ratio of intensity at 660 nm to that at 615 nm was plotted against the intensity at 660 nm. Cells with the highest ratio and sufficient intensity at 660 nm were collected (Fig. 1*B*). Usually one million cells were collected each time, and they were grown in the absence of doxycycline until 24 h before the next round of sorting.

Mutant Characterization. Sorted cells were amplified in the absence of doxycycline, and 0.1 μg/ml doxycycline was then added for 10 h. Total mRNA was extracted from these cells and used as template for RT-PCR to clone mRFP mutant DNA with primer pair pCL5 (5′-AGCTCGTTTAGTGAACCGTCA-GATC-3′) and pCL3 (5′-GGTCTTTCATTCCCCCCCTTTT-TCTGGAG-3′). These mutant mRFP genes were subcloned into a pBAD vector (Invitrogen) and expressed in *Escherichia coli*. A His-6 tag was added to the C terminus to facilitate protein purification using Ni-NTA chromatography (Qiagen, Valencia, CA). Spectroscopic measurements were as described previously (12), except that concentrations of mRFPs were determined by assuming an extinction coefficient after denaturation in 0.1 M NaOH of 44,000 $M^{-1} \cdot cm^{-1}$ at 452 nm, the same value as that of similarly denatured *Renilla* GFP (13, 14).

Photobleaching Measurements. Microdroplets of aqueous protein, pH 7.4, typically 5–10 μm in diameter, were created on a
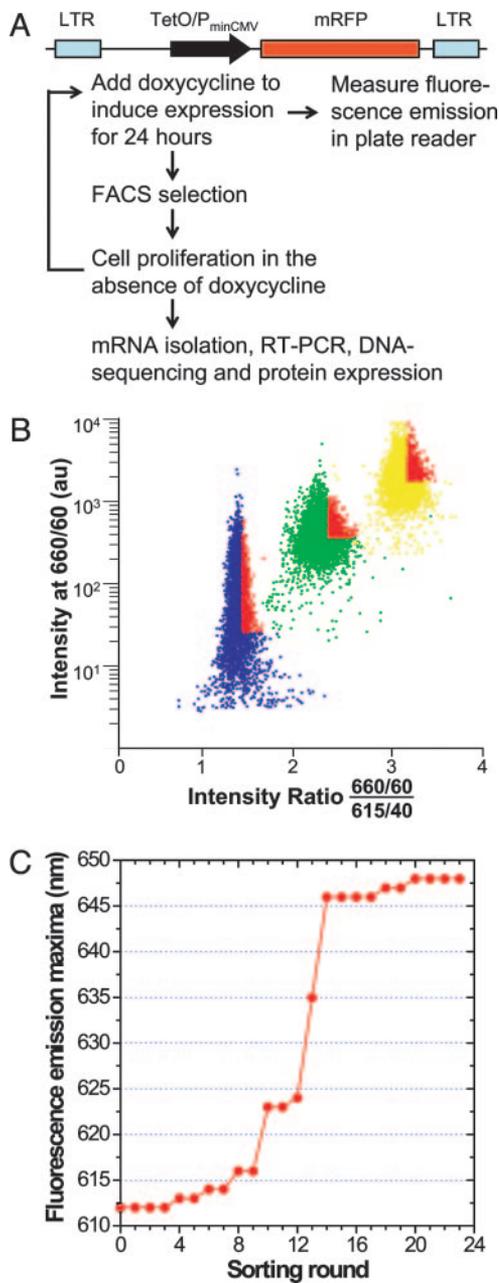

Freely available online through the PNAS open access option.

Abbreviations: SHM, somatic hypermutation; mRFP, monomeric red fluorescent protein.

APPLIED BIOLOGICAL SCIENCES

Fig. 1. Directed evolution of mRFP with red-shifted emission by SHM in Ramos cells. (*A*) Schematic illustration of the construct and evolutionary process. TetO/P$_{minCMV}$, Tet operator/minimal CMV promoter. (*B*) Typical FACS criteria for ratio sorting. Ramos cells were excited at 568 nm, and two emission filters (660/60 and 615/40) were used. The ratio of intensity at 660 nm to that at 615 nm was plotted against the intensity at 660 nm. Cells with the highest ratio and sufficient intensity at 660 nm were collected each time, and they were grown in the absence of doxycycline until 24 h before the next round of FACS. Cell populations from rounds 1, 10, and 20 are shown in blue, green, and yellow, respectively. Collected cells are highlighted in red. au, Arbitrary unit. (*C*) Fluorescence emission maxima of the Ramos cell population in each round, measured with a spectrofluorometric plate reader (Safire, Tecan, Maennedorf, Switzerland).

microscope coverslip under mineral oil and bleached by using a Zeiss Axiovert 200 microscope at 14.3 W/cm^2 with a 75-W xenon lamp and a 540- to 595-nm excitation filter. Reproducible results required preextraction of the mineral oil with aqueous buffer shortly before microdroplet formation.
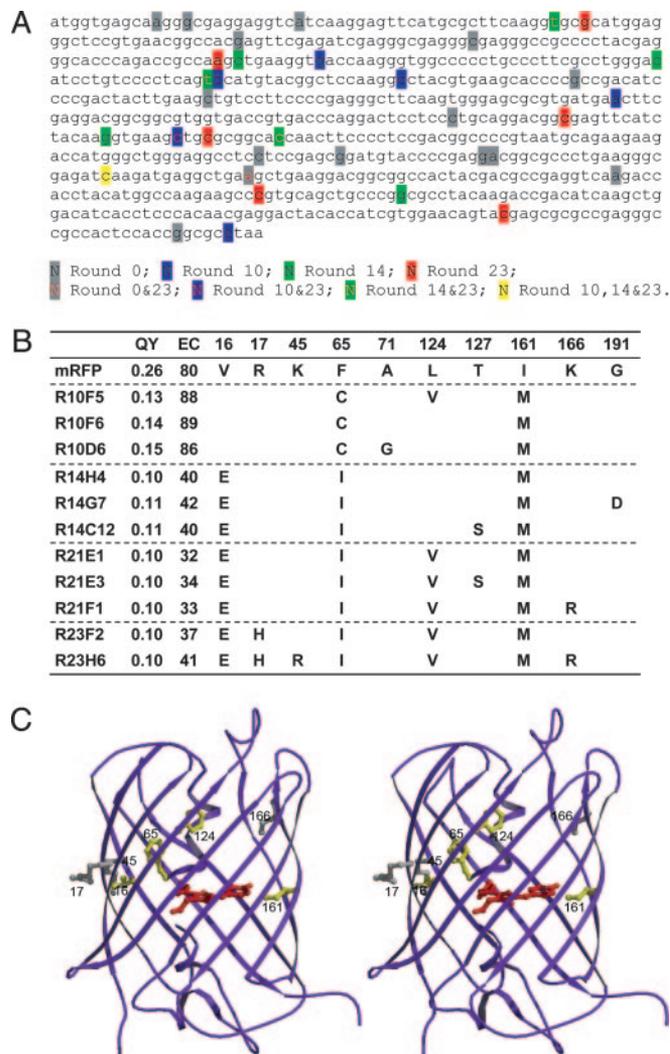
Fig. 2. Evolution pathway of the mutants. (*A*) Nucleotides mutated by SHM in different rounds. Twenty random samples were sequenced in round 0, 8 in round 10, 8 in round 14, and 12 in round 23. (*B*) Amino acid mutations, quantum yields (QY), and extinction coefficients (EC) of different mutants. R10F5 represents mutant F5 from round 10. We named mutants R10D6 and R23H6 mRaspberry and mPlum, respectively. (*C*) Stereoview of mutation loci in mPlum based on the crystal structure of DsRed. The chromophore of RFP is shown in red. Residues are highlighted in yellow for emission-shift mutations and in gray for neutral mutations.

Identification of Integration Loci.

The integration loci of provirus in the Ramos genome was determined by using reverse PCR as described (15), except that the secondary PCR products were directly sequenced without further cloning after agarose gel electrophoresis and purification. *Bam*HI and *Sau*3AI were used to digest genomic DNA separately. The primary PCR primer pairs were as follows: LW131 (5′-GACAGCTTCAAG-TAGTCGGGGATG-3′) and LW132 (5′-CTTCCCCG AGGGCTTCAAGTGGG-3′) for *Bam*HI cloning; and LW128 (5′-CGAACAGAAGCGAGAAGCGAAC-3′) and LW129 (5′-CGCGCTTCTGCTCCCCGAGCTC-3′) for *Sau*3AI cloning. The secondary PCR primer pairs were as follows: LW130 (5′-TCGCCCTTGCTCACCATGGTGGC-3′) and LW127 (5′-GCCAGTCCTCCGATTGACTGAGTC-3′) for *Bam*HI cloning; and LW126 (5′-CACCCTGGAAACATCTGATGGTTC-3′) and LW127 for *Sau*3AI cloning. Sequences were compared with EST databases by using BLASTN (www.ncbi.nlm.nih.gov),
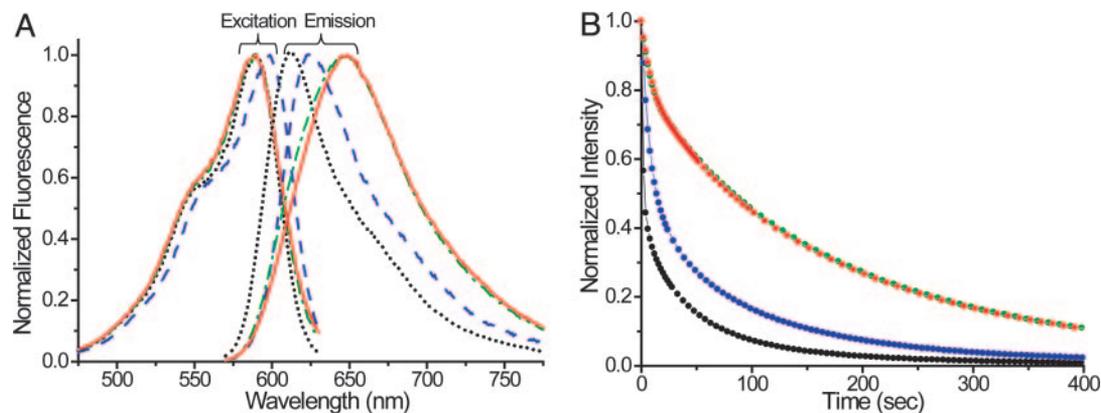
Fig. 3. Characterization of evolved mutant proteins. (*A*) Fluorescence spectra of purified parental mRFP1.2 protein and representative mutant proteins from different rounds. Black dot, mRFP1.2; blue dash, mRaspberry; green dash dot, R14H4; red solid line, mPlum. In rounds 22 and 23, brighter cells were sorted while maintaining the ratio. Thus, mutants from rounds 21 and 23 have similar fluorescence spectra, except that round 23 mutants have larger extinction coefficients. All emission spectra were taken at the excitation wavelength 564 nm, and emission was monitored at 640 nm for excitation spectra. (*B*) Fluorescence intensity decay during photobleaching was at 14.3 W/cm² at 568 nm. Color code is as in *A*.

and all matching sequences had BLASTN probability values of $<10^{-61}$.

Results and Discussion

SHM Introduces Mutations into an Exogenous, Non-Ig Gene. The gene for mRFP1.2 (10) was expressed as a single copy in Ramos under the control of a doxycycline-inducible promoter, Tet-on (Fig. 1*A*), so that SHM could be controlled by varying the transcription level. First, fluorescent cells were enriched by using six rounds of FACS of cells to which 2 μg/ml doxycycline was added 24 h before each round to induce mRFP expression. A fluorescent cell population was established with >96% cells fluorescent. Sequencing of different clones revealed many mutations with features of SHM scattered throughout the target gene (Fig. 2*A*, Round 0). Of 20 samples sequenced, 12 had 1–3 mutations. Starting from this fluorescent population, >15% of cells lost fluorescence when doxycycline was added for 120 h, whereas <5% lost fluorescence when doxycycline was present for only 24 h, suggesting that more transcription generated more mutations. In control HEK293 cells lacking SHM, a similarly established fluorescent population did not change its fluorescence significantly upon such treatment.

Evolution of mRFP Mutants with Far-Red-Shifted Emissions. We next tested whether an mRFP with red-shifted emission could be evolved directly in Ramos. The parental mRFP1.2 fluoresces with a peak at 612 nm. A longer wavelength emission would confer greater tissue penetration and spectral separation from autofluorescence and other fluorescent proteins. In each round of sorting, we collected ≈5% of the population having the highest ratio of 660-nm to 615-nm emissions yet maintaining at least a minimum brightness at the former (Fig. 1*B*). Over 23 rounds of sorting and regrowth, the emission maxima shifted to longer wavelengths in several steps (Fig. 1*C*). After each major step, mutant mRFP genes were isolated, sequenced (Fig. 2), and transferred to a standard bacterial expression system so that mutant proteins could be purified in larger quantities and characterized (Fig. 3*A*).

The mutant with the longest emission wavelength (dubbed "mPlum" in view of its monomeric nature, purplish appearance by reflected light, and deep red glow) peaked at 649-nm emission, 37 nm longer than the peak of the original mRFP1.2 and 12 nm beyond the previous furthest-red emitter, the tandem dimer t-HcRed1 (16). The absorbance and excitation maxima of mPlum remained at 590 nm, surprisingly unchanged from those

of mRFP1.2 and identical to those of t-HcRed1. The 59-nm Stokes' shift is unusually large. The fluorescence quantum yield of mPlum (0.10) is somewhat lower than that of mRFP1.2 (0.25) but still well above that of t-HcRed (0.04). The far-red emission of mPlum will be useful for improving optical imaging in intact mammals (17), especially of chimeric proteins and genetically encoded indicators (18) where it is essential that the fluorescent protein be monomeric. The largest wavelength of excitation (598 nm), extinction coefficient (86,000 M⁻¹·cm⁻¹), and quantum yield (0.15) were found in a round 10 mutant, "mRaspberry," whose emission maximum was 625 nm. The times for 50% maturation of mPlum and mRaspberry are ≈100 and ≈55 min, respectively.

Furthermore, all evolved mutants were considerably more resistant to photobleaching than the parental mRFP1.2. When exposed to a 14.3-W/cm² beam at ≈568-nm light on a microscope stage, microdroplets of mPlum and mRaspberry under oil took 80 and 14 s, respectively, to bleach to 50% of initial intensity, 30- and 5.2-fold longer than mRFP1.2 (Fig. 3*B*). The repeated FACS selection for cells exceeding a minimum brightness might have promoted photostability by discriminating against mutants that bleached significantly during the passage through the intense laser excitation spot.

Analysis of SHM Evolution Pathway. DNA sequences of these mutants revealed the evolution pathway. New mutations, including silent ones, were generated in each round (Fig. 2*A*), indicating that SHM does not stall but keeps exploring the sequence space. Within a round, different clones shared common mutations, such as F65C and I161M in round 10 (Fig. 2*B*). Beneficial mutations were preserved from round to round, such as I161M and V16E. Although thymine is not favored for SHM (5), it was mutated to guanine or adenine in the F65 codon to generate cysteine and isoleucine, respectively, and to adenine in the V16 codon to generate glutamic acid. These results indicate that beneficial mutations can be found although they may be relatively disfavored by SHM's known biases for particular base changes.

Comparison of mutations with phenotypes indicates that alterations at positions 16 and 65 gave rise to the dramatic red shift of the emission peak, whereas mutations at positions 124 and 161 mainly narrowed the emission width by shrinking the short-wavelength side of the peak. The latter is a subtle beneficial effect that is usually difficult to achieve. When mapped on the crystal structure of DsRed (19), from which mRFP was derived

(Fig. 2C), residue 65 just precedes the chromophore. Residues 16 and 161 are located at opposite ends of the chromophore with side chains facing it. Residue 124 also faces inward, toward the helix bearing the chromophore. Mutation of these residues could directly perturb the chromophore's microenvironment, resulting in emission shift. In contrast, residues 17, 45, and 166 face away from the chromophore, and thus their major contribution is to improve protein folding and brightness.

Parallel experiments using random mutagenesis or rational design based on crystal structure have not yet generated mRFP mutants with emission maxima of >632 nm, suggesting that SHM can solve challenging problems in global searching. So far, all wild-type members of this chromoprotein superfamily with absorbance maxima of >570 nm have been nonfluorescent tetramers rather than fluorescent monomers (20, 21), so a few months of SHM and FACS accomplished what billions of years of evolution in coral reefs apparently has not.

More detailed evidence for the power of SHM is that traditional *in vitro* saturation mutagenesis at each locus identified by SHM produced no further increase in emission wavelengths. Instead, most mutations resulted in either fluorescence loss or blue shift. For example, the emission spectra in Fig. 4 *A* and *B* show that SHM found the optimum substitutions at positions 65 and 124, respectively. Saturation mutation results for positions 16 and 17 (16/17) and positions 161 and 166 (161/166) are tabulated in Fig. 4C. Furthermore, several residues such as T127 were mutated in some but not all SHM clones. Saturation mutagenesis at these loci indicated that they are neutral; i.e., they do not affect emission wavelength (Fig. 4B). In addition, saturation mutagenesis was performed on residues 16 and 65 simultaneously to test whether a better combination exists to afford longer emission. Again, all mutational combinations different from that found by SHM led to fluorescence loss or blue shift. These results suggest that our method can identify and locally optimize critical residues to cope with selection pressure.

Integration Loci of Target Gene in Ramos Genome. Whether SHM is locus-specific for the IgV gene is under debate. We determined the integration loci of the mRFP mutant gene in several representative rounds of FACS-selected cells. In round 2, the target gene was mainly found in chromosomes 5, 16, 18, and 20, which do not contain Ig genes. The multiple-site distribution is expected because retrovirus integrates into host genome rather randomly. Mutations with the characteristics of SHM were found in the target gene as early as round 0 with high frequency (12 of 20 sequenced clones had mutations). However, by round 23, when mPlum was isolated, only a single integration site was found, at the Ig heavy-chain locus in chromosome 14 between gene *IgHV7-34-1* and *IgHV4-34*. These results show that SHM can mutate exogenous genes integrated at many loci in the genome (8), but the mutation rate may be higher at the Ig loci. Therefore, desired properties requiring multiple mutations are more likely generated from a clone with the target gene integrated at Ig loci. In future applications, it would be more efficient to direct the target gene to such loci to jump-start the evolution. Such targeting should not be difficult, because universal gene replacement vectors working at Ig loci have been generated previously (22).

Sequence Space Sampled by SHM. Although only seven mutations are needed to convert mRFP1.2 to mPlum, the sequence space that SHM has to sample to reach this final status presumably should be much larger, because many mutations, alone or combined, are deleterious to fluorescence intensity, emission, and protein folding. The 3′ LTR of the retrovirus vector used to introduce the mRFP gene into the Ramos genome can serve as an internal reference for the cumulative effect of SHM unbiased by phenotypic selection. We sequenced the very end of the 3′
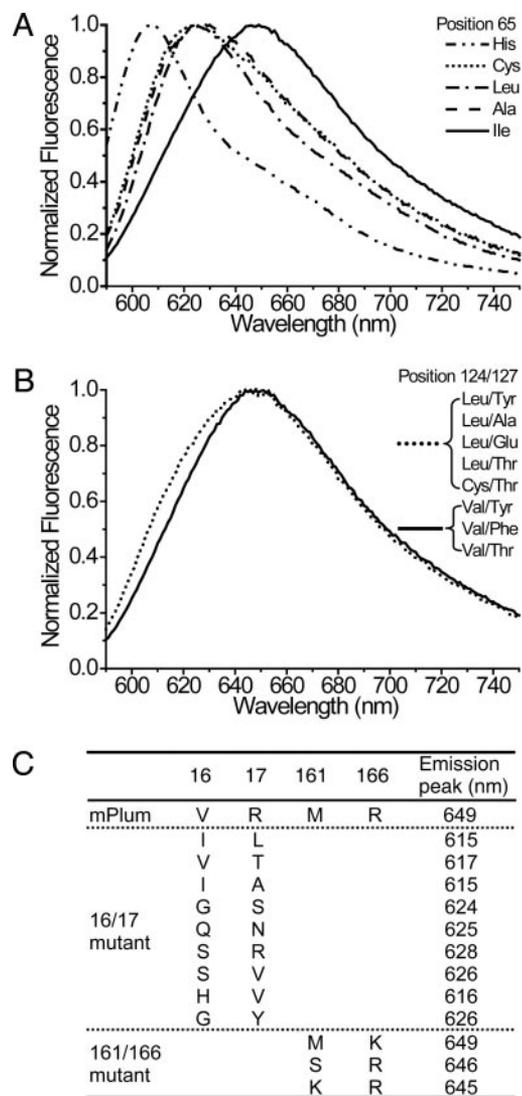
Fig. 4. Saturation mutagenesis analysis of positions identified by SHM in mPlum. (*A*) Fluorescence emission spectra of mutants with different mutations at position 65. All mutations other than the SHM-identified isoleucine dramatically blue-shift the emission. (*B*) Fluorescence emission spectra of mutants with different mutations at positions 124 and 127. Mutations at position 124 other than the SHM-identified valine broaden the emission peak to the short-wavelength side. Regardless of the mutations at position 127, mutants with leucine or cysteine at position 124 overlap, and mutants with valine at position 124 also overlap. (*C*) Fluorescence emission peaks of mPlum mutants with different mutations at positions 16 and 17 and positions 161 and 166. For saturation mutagenesis at positions 16 and 17, representative mutants with emission spanning from 614 to 649 nm were sequenced. For saturation mutagenesis at positions 161 and 166, only mutants with emissions of >640 nm were sequenced. Of 15 sequenced samples, methionine/lysine was found in 11 clones and serine/arginine in 2 clones.

LTR in mPlum and two randomly picked clones in round 2 and compared them with the original sequence in the parental vector (Fig. 5). Among 117 sequenced nucleotides, the 3′ LTR in mPlum has 15 mutations including an insertion, whereas there is only one mutation in two clones from round 2. The high mutation frequency indicates that SHM indeed samples a large sequence space.

Conclusion

SHM of non-Ig genes is no longer limited to repairing artificial defects but can accumulate multiple reinforcing mutations

```
Vector          1  CGGGTACCCGTGTATCCAATAAACCCTCTTGCAGTT-GCATCCGACTTGTGGTCTCGCTG
Round 2 clone 1 1  CGGGTACCCGTGTATCCAATAAACCCTCTTGCAGTT-GCATCCGACTTGTGGTCTCGCTG
Round 2 clone 2 1  CGGGTACCCGTGTATCCAATAAACCCTCTTGCAGTT-GCATCCGACTTGTGGTCTCGCTG
mPlum           1  CGGGTACCCGTATTCCAATAAAGCCTCTTGCTGTTTGCATCCGAATCGTGGTCTCGCTG

Vector          60 TTCCTTGGGAGGGTCTCCTCTGAGTGATTGACTACCCGTCAGCGGGGGTCTTTCATT
Round 2 clone 1 60 TTCCTTGGGAGGGTCTCCTCTGAGTGATTGACTACCCGTCAGGGGGGTCTTTCATT
Round 2 clone 2 60 TTCCTTGGGAGGGTCTCCTCTGAGTGATTGACTACCCGTCAGCGGGGGTCTTTCATT
mPlum           61 TTCCTTGGGAGGGTCTCCTCTGAGTGATTGACTACCCACGACGGGTAGTCTTTCATT
```

Fig. 5. Sequence alignments of the end of 3′ LTR from the retroviral vector, two clones of round 2, and mPlum. Mutations are shaded in black.

throughout the gene to produce new and desirable phenotypes difficult or impossible to find by conventional mutagenesis. SHM-mediated protein evolution in live cells obviates labor-intensive *in vitro* mutagenesis and screening, samples a large protein space, and directly links genotypes to cell phenotypes. An engineered error-prone DNA polymerase I can perform somewhat analogous targeted mutagenesis on multicopy ColE1 plasmids in bacteria (23), but SHM works on single-copy integrants in well established mammalian cell lines, which are indispensable for the study of many eukaryotic proteins such as therapeutic targets. SHM should provide a general strategy to iteratively accumulate multiple desirable mutations in many other proteins whose function can be robustly assessed by high-throughput selections and screens that leave the desired cells alive. Catalytic antibodies (24) have been the showcase for using the immune system to evolve functions remote from immunology, but the repertoire of useful B cell creativity has now further expanded to proteins unrelated to antibodies.

1. Minshull, J. & Stemmer, W. P. C. (1999) *Curr. Opin. Chem. Biol.* **3,** 284–290.
2. Petrounia, I. P. & Arnold, F. H. (2000) *Curr. Opin. Biotechnol.* **11,** 325–330.
3. Greener, A., Callahan, M. & Jerpseth, B. (1997) *Mol. Biotechnol.* **7,** 189–195.
4. Papavasiliou, F. N. & Schatz, D. G. (2002) *Cell* **109,** Suppl., S35–S44.
5. Martin, A. & Scharff, M. D. (2002) *Nat. Rev. Immunol.* **2,** 605–614.
6. Neuberger, M. S., Harris, R. S., Di Noia, J. & Petersen-Mahrt, S. K. (2003) *Trends Biochem. Sci.* **28,** 305–312.
7. Bachl, J., Carlson, C., Gray-Schopfer, V., Dessing, M. & Olsson, C. (2001) *J. Immunol.* **166,** 5051–5057.
8. Wang, C. L., Harper, R. A. & Wabl, M. (2004) *Proc. Natl. Acad. Sci. USA* **101,** 7352–7356.
9. Rajewsky, K., Forster, I. & Cumano, A. (1987) *Science* **238,** 1088–1094.
10. Campbell, R. E., Tour, O., Palmer, A. E., Steinbach, P. A., Baird, G. S., Zacharias, D. A. & Tsien, R. Y. (2002) *Proc. Natl. Acad. Sci. USA* **99,** 7877–7882.
11. Sale, J. E. & Neuberger, M. S. (1998) *Immunity* **9,** 859–869.
12. Baird, G. S., Zacharias, D. A. & Tsien, R. Y. (2000) *Proc. Natl. Acad. Sci. USA* **97,** 11984–11989.
13. Ward, W. W. (1998) in *Green Fluorescent Protein: Properties, Applications, and Protocols*, eds. Chalfie, M. & Kain, S. (Wiley, New York), pp. 45–75.
14. Gross, L. A., Baird, G. S., Hoffman, R. C., Baldridge, K. K. & Tsien, R. Y. (2000) *Proc. Natl. Acad. Sci. USA* **97,** 11990–11995.
15. Li, J., Shen, H., Himmel, K. L., Dupuy, A. J., Largaespada, D. A., Nakamura, T., Shaughnessy, J. D., Jr., Jenkins, N. A. & Copeland, N. G. (1999) *Nat. Genet.* **23,** 348–353.
16. Fradkov, A. F., Verkhusha, V. V., Staroverov, D. B., Bulina, M. E., Yanushevich, Y. G., Martynov, V. I., Lukyanov, S. & Lukyanov, K. A. (2002) *Biochem. J.* **368,** 17–21.
17. Ray, P., De, A., Min, J. J., Tsien, R. Y. & Gambhir, S. S. (2004) *Cancer Res.* **64,** 1323–1330.
18. Zhang, J., Campbell, R. E., Ting, A. Y. & Tsien, R. Y. (2002) *Nat. Rev. Mol. Cell Biol.* **3,** 906–918.
19. Yarbrough, D., Wachter, R. M., Kallio, K., Matz, M. V. & Remington, S. J. (2001) *Proc. Natl. Acad. Sci. USA* **98,** 462–467.
20. Gurskaya, N. G., Fradkov, A. F., Terskikh, A., Matz, M. V., Labas, Y. A., Martynov, V. I., Yanushevich, Y. G., Lukyanov, K. A. & Lukyanov, S. A. (2001) *FEBS Lett.* **507,** 16–20.
21. Verkhusha, V. V. & Lukyanov, K. A. (2004) *Nat. Biotechnol.* **22,** 289–296.
22. Kardinal, C., Selmayr, M. & Mocikat, R. (1996) *Immunology* **89,** 309–315.
23. Camps, M., Naukkarinen, J., Johnson, B. P. & Loeb, L. A. (2003) *Proc. Natl. Acad. Sci. USA* **100,** 9727–9732.
24. Schultz, P. G., Yin, J. & Lerner, R. A. (2002) *Angew. Chem. Int. Ed.* **41,** 4427–4437.

APPLIED BIOLOGICAL SCIENCES